Journal of Nuclear Materials 415 (2011) S777–S780

Contents lists available at ScienceDirect

Journal of Nuclear Materials

journal homepage: www.elsevier.com/locate/jnucmat

Surface chemistry and physics of deuterium retention in lithiated graphite

C.N. Taylor [a,b,*], J.P. Allain [a,b], B. Heim [a,b], P.S. Krstic [c], C.H. Skinner [d], H.W. Kugel [d]

[a] Purdue University, West Lafayette, IN 47907, USA
[b] Birck Nanotechnology Center, Discovery Park, Purdue University, West Lafayette, IN 47907, USA
[c] Oak Ridge National Laboratory, Oak Ridge, TN 37831, USA
[d] Princeton Plasma Physics Laboratory, Princeton, NJ 08543, USA

ARTICLE INFO

Article history:
Available online 8 October 2010

ABSTRACT

Lithium wall conditioning in TFTR, CDX-U, T-11M, TJ-II and NSTX is found to yield enhanced plasma performance manifest, in part, through improved deuterium particle control. X-ray photoelectron spectroscopy (XPS) experiments examine the affect of D irradiation on lithiated graphite and show that the surface chemistry of lithiated graphite after D ion bombardment (500 eV/amu) is fundamentally different from that of non-Li conditioned graphite. Instead of simple LiD bonding seen in pure liquid Li, graphite introduces additional complexities. XPS spectra show that Li–O–D (533.0 ± 0.6 eV) and Li–C–D (291.4 ± 0.6 eV) bonds, for a nominal Li dose of 2 μm, become "saturated" with D at fluences between 3.8 and 5.2 × 10^{17} cm^{-2}. Atomistic modeling indicate that Li–O–D–C interactions may be a result of multibody effects as opposed to molecular bonding.

1. Introduction

Fusion devices such as TFTR, CDX-U, FTU, T-11M, TJ-II and NSTX have found improvements in plasma performance through lithium wall conditioning. Improvements include edge localized mode (ELM) reduction, reduction in lower divertor C and O luminosity, and deuterium particle control [1,2]. Previous work has shown that pure liquid lithium allows for full uptake of incident deuterium ions to form LiD [3]. Post-mortem NSTX tiles and control studies show that lithiated graphite reacts readily with oxygen to form additional chemical bonds, including lithium-peroxide and lithium-carbonate [4].

Recent experiments at Purdue University examine the effect of deuterium irradiation on lithiated graphite [5]. XPS data show interactions between Li–O at 530.0 ± 0.6 eV, Li–O–D at 533.0 ± 0.6 eV, and Li–C–D manifest at 291.4 ± 0.6 eV. Deuterium related bonds Li–O–D and Li–C–D (also represented stoichiometrically as $Li_xO_yD_{1-x-y}$ and $Li_xC_yD_{1-x-y}$) are found to intensify relative to non-deuterium related bonds Li–O and Li–C–X (Li_xO_y and $Li_xC_yD_{1-x-y}$) as deuterium fluence increases. While stoichiometric formulas are conceivable, it will be shown that it is more probable for Li, C, O, and D to interact as multibody complexes as opposed to molecular bonds. Thus, Li–O represents a statement on coupling between Li and O rather than the LiO molecule.

As deuterium interacts with lithiated graphite, for high fluences (10^{18} cm^{-2}) it is anticipated that the intensity of deuterium related bonds will grow relative to non-deuterium related bonds. It is also logical that this ratio will reach some saturation level, and this saturation level corresponds to the point at which deuterium retention diminishes. The relative comparison of deuterium and non-deuterium related bonds is analyzed and discussed presently. Deuterium retention is of significant importance for fusion devices since an understanding of deuterium saturation of lithiated graphite can provide insite on lithium wall conditioning.

2. Experimental setup

Full experimental procedures have been discussed in detail elsewhere [5]. In brief, samples are fabricated from ATJ graphite and sized to 10.25 mm or 12.5 mm diameter samples 2–3 mm in thickness. ATJ graphite, nominally polycrystalline, is used in experiments as it is the primary plasma-facing component (PFC) in NSTX. Highly ordered pyrolytic graphite (HOPG) is also used as a substrate material for control experiments and is chosen because of its high purity, laminar crystalline surface.

Deposition of 2 μm of lithium results in a 6.5% error according to cross-calibration with microbalance and SEM analysis. This is only a nominal thickness given the porous morphology of ATJ graphite surfaces. After lithium deposition, samples are irradiated using an Omicron ISE-10 low-energy ion source (500 eV/amu) at a deuterium ion flux of ~10^{13} cm^{-2} s^{-1}. Samples are transferred *in-vacuo* for XPS to assess the chemical state of the surface prior to and following each process (i.e. deposition and irradiation). X-rays are produced using a non-monochromatic, non-charge compensating Al/Mg K-alpha source. Error in XPS spectra

* Corresponding author at: 400 Central Drive, West Lafayette, IN 47907, USA
E-mail address: ctaylor@purdue.edu (C.N. Taylor).

0022-3115/$ - see front matter © 2010 Elsevier B.V. All rights reserved.
doi:10.1016/j.jnucmat.2010.09.049

originates from equipment resolution (0.6 eV) and statistical standard error (SE). Typically our spectra has SE < 0.02 eV and, relative to the resolution, does not contribute significantly in error propagation.

3. Results and discussion

3.1. General peak behavior

The chemical state of graphite after lithium deposition and deuterium irradiation is discussed in detail elsewhere and only a summary of those results is presented here [5]. XPS of virgin graphite shows a primary peak at 283.6 ± 0.6 eV and 532.0 ± 0.6 eV, and corresponds to graphitic and CO bonds, respectively (Figs. 1 and 2 labeled 'Virgin'). Deviations from standard XPS libraries [6] are a result of a non-charge compensated X-ray source. Lithium deposition produces an additional peak in the O1s spectrum, that is not apparent for virgin graphite, at 529.5 ± 0.6 eV and is attributed to Li–O (see Fig. 1, 'Li-2 μm'). Deuterium irradiation shifts the Li–O peak to 530.1 ± 0.6 eV, and an additional peak forms at 533.0 ± 0.6 eV which is attributed to Li–O–D (or preferred interactions between Li, O and D). In the C1s spectrum, 2 μm lithium deposition "buries" the graphite and suppresses the graphitic peak as seen in Fig. 2 labeled 'Li-2 μm'. Peak suppression is apparent in

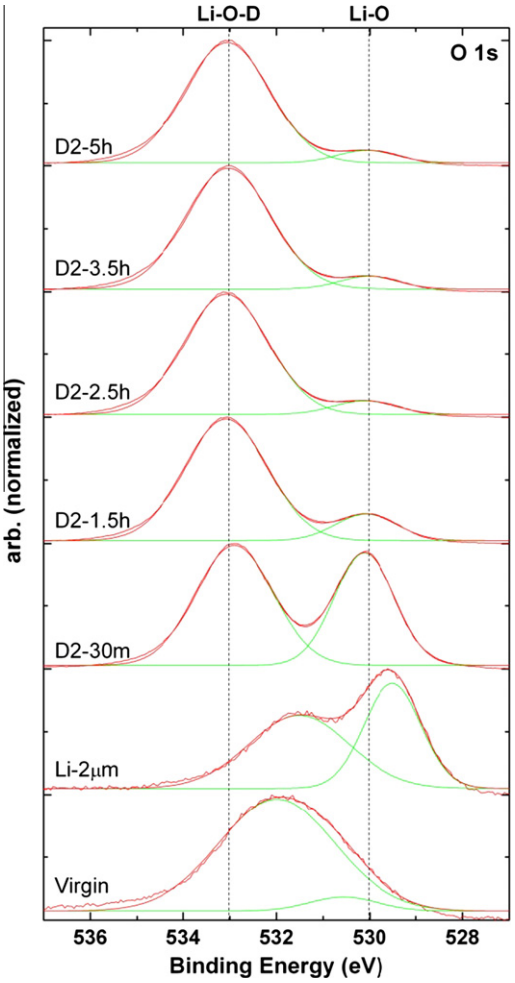

Fig. 1. XPS O1s spectra of virgin graphite (ATJ147), after 2 μm lithium deposition, and after D_2 irradiation fluences: 30 min (9.0×10^{17} cm^{-2}), 1.5 h (2.5×10^{17} cm^{-2}), 2.5 h (3.8×10^{17} cm^{-2}), 3.5 h (5.2×10^{17} cm^{-2}), and 5.0 h (7.2×10^{17} cm^{-2}). Note that the Li–O peak (530.1 eV ± 0.6 eV) diminishes as the Li–O–D peak intensifies (at 533.0 ± 0.6 eV).

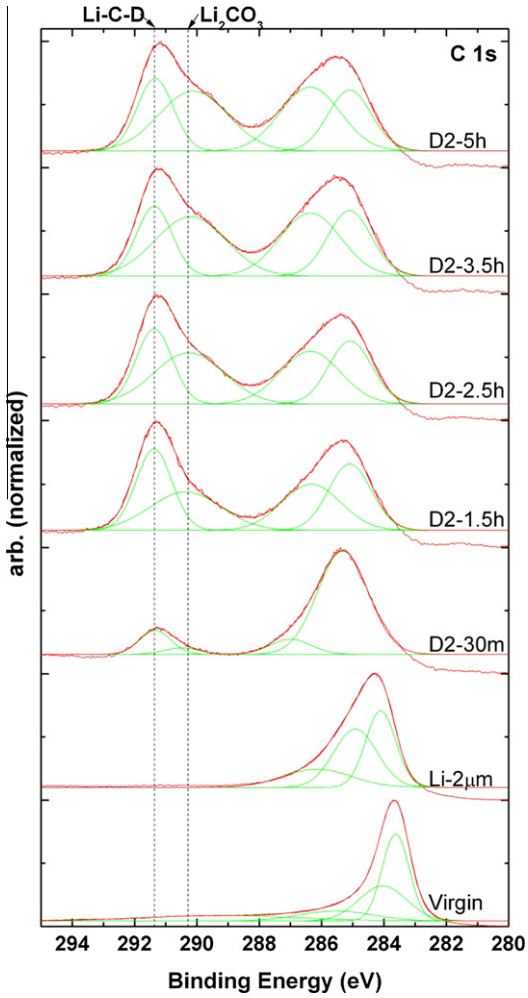

Fig. 2. XPS C1s spectra of virgin graphite (ATJ147), post 2 μm lithium deposition, and after D_2 irradiation fluences: 30 min (9.0×10^{17} cm^{-2}), 1.5 h (2.5×10^{17} cm^{-2}), 2.5 h (3.8×10^{17} cm^{-2}), 3.5 h (5.2×10^{17} cm^{-2}), and 5.0 h (7.2×10^{17} cm^{-2}).

the pre-normalized spectrum (not shown) and is observed as a decrease in intensity. Deuterium irradiation induces a peak positioned at 291.4 ± 0.6 eV and is attributed to Li–C–D. Exposing lithiated graphite to air results in a strong Li_2CO_3 peak at 290.3 ± 0.6 eV [4].

In addition, previous work has examined NSTX post-mortem tiles to assess surface chemistry from fusion devices. Following a cleaning procedure of Ar sputtering and annealing, NSTX post-mortem tiles showed XPS peaks identical (±0.6 eV) to Li–O, Li–O–D, and Li–C–D peaks observed in control experiments.

3.2. Li–D saturation in oxygen peaks

After 30 min deuterium irradiation (9.0×10^{17} cm^{-2}), the Li–O–D and Li–O peak heights are nearly equal in magnitude ('D2-30' in Fig. 1). The spectrum is deconvoluted into two Gaussian peaks, and by integration the individual peak areas are computed. The area ratio of Li–O–D and Li–O after 30 min deuterium irradiation is 0.8. However, as the deuterium fluence increases over additional irradiations, this ratio increases. After 5 h deuterium irradiation (7.2×10^{17} cm^{-2}), the Li–O–D/Li–O ratio is 14:1. This suggests the formation of Li–O–D consumes available Li–O. The growth of this ratio, however, does not increase indefinitely because there is not an indefinite supply of Li–O available to interact with deuterium. Consequently, the Li–O–D/Li–O ratio is found to have a

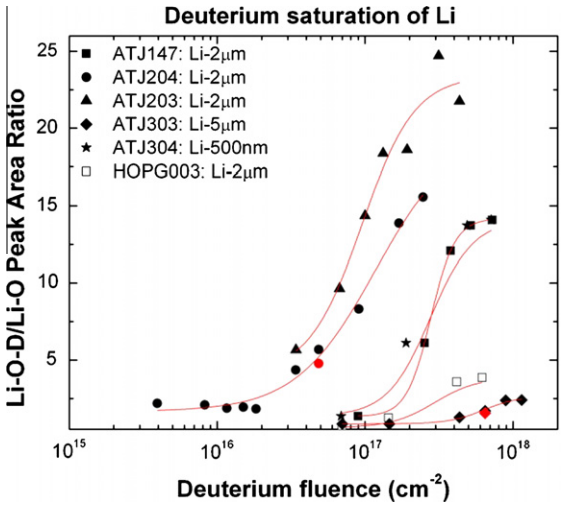

Fig. 3. Ratio of Li–O–D area to Li–O area with respect to deuterium fluence. The fluence at which the ratio ceases to change indicates that deuterium is inducing a lesser effect.

growth threshold beyond which increasing the deuterium fluence does not lead to an increase in the XPS peak associated with preferred Li–O–D interactions. This fluence-dependent saturation has been plotted for various samples and is shown in Fig. 3.

A logistic growth rate fit is applied to the data in Fig. 3 showing minimum and maximum plateaus. Here deuterium saturation is defined as the fluence at which the Li–O–D/Li–O area ratio changes <10% between consecutive irradiations (a normalized derivative). For sample ATJ147 (from which data in Figs. 1 and 2 were taken), deuterium saturation occurs at 5.2×10^{17} cm^{-2}. The average saturation fluence for samples with 2 μm deposited lithium is $2.9 \times 10^{17} \pm 1.7 \times 10^{17}$ cm^{-2}. Comparing this saturation fluence to the average NSTX wall ion fluence ($\sim 10^{17}$ cm^{-2}) would indicate that the 10–100s of nm lithium deposited between shots [2] most likely saturates after a single discharge.

This experiment was repeated for a nominal lithium thickness of 500 nm and saturation was found to occur at a fluence of 7.1×10^{17} cm^{-2}, which is higher than the average saturation fluence for 2 μm lithium. One potential implication is that 500 nm and 2 μm lithium are capable of retaining equal amounts of lithium. This could be possible if both thicknesses fully intercalate into the graphite leaving only monolayer coverage at the surface. For a sample with 5 μm deposited lithium, saturation is found to occur at 1.1×10^{18} cm^{-2}. This indicates that for 5 μm, more surface lithium is available to interact with deuterium. Lithium intercalation in graphite is well documented and causes lithium to diffuse away from the free surface [7]. Intercalation occurs for each of our samples (500 nm, 2 μm, and 5 μm lithium), however, at the time of analysis, the sample with 5 μm lithium may have more Li remaining on the surface available for binding.

Questions remain regarding the state of implanted deuterium atoms after saturation. For ion-solid sputtering of a two-component system, preferential sputtering occurs and is proportional to the two components atomic concentration ratio and a preferential sputtering coefficient [8]. If lithiated graphite became completely saturated, introducing additional deuterium ions could have several affects. First, it would break bonds between Li, O, C, and D leading to "dangling bonds" of these elements and thus liberate them for additional bonding. Second, deuterium ions would preferentially sputter Li, O, C, and D according to each atomic concentration and their respective preferential sputtering constants. More importantly, chemical-sputtering would likely dominate given the reactivity of several species involved (e.g. C, D, Li and O) [9].

3.3. Li–D saturation in carbon peaks

XPS C1s peaks are inherently more complicated than the O1s peaks due to the increased number of deconvoluted peaks in this spectrum. For the present analysis, the development of new peaks resultant from deuterium irradiation is of primary interest as they may elucidate on the fundamental interaction of deuterium and the lithiated graphite matrix. Fig. 2 shows that after 9.0×10^{17} cm^{-2} initial deuterium irradiation ('D2-30 m') a new peak forms at 291.4 ± 0.6 eV and this peak is attributed to Li–C–D [5]. At the maximum irradiation fluence of 7.2×10^{17} cm^{-2} ('D2-5 h'), the Li–C–D peak intensifies and becomes more broad. Li_2CO_3 contributes to the broadness of this peak, and graphitic (C) and CO (or CO–X) bonds are found to contribute to the lower energy peaks (283–287 eV) [4]. Here, the contribution of CO to the total peak varies with fluence, thus indicating that it is dependent on deuterium irradiation. It is presently unknown whether changes in CO (286.5 ± 0.6 eV) are a result of physical sputtering or chemical sputtering. Precautionary to the latter, it has been labeled as CO–X, indicating that an element X could be influential. After deuterium irradiation, the C1s spectrum can be deconvoluted into at least four distinct peaks, therefore it is prudent to consider each peak independently. Taking ratios in the O1s spectrum was appropriate as only two peaks were present after deuterium irradiation.

The integrated peak area for each of the four C1s deconvoluted peaks, divided by the total C1s peak area, is plotted with respect to fluence and is shown in Fig. 4. Previously, saturation was used to explain how Li–O converted to Li–O–D with deuterium irradiation. In the C1s spectrum it is not yet apparent that a single peak (i.e. Li–C) converts into Li–C–D following irradiation. Consequently, it would be erroneous to say that Li–C–D saturates since saturation implies some knowledge of the base source. Instead, the plateau in C1s peaks is identified as stagnation and is mathematically defined similar to saturation.

Results in Fig. 4 shows that the C surface concentration decreases while other carbon bonds (Li_2CO_3 and Li–C–D) each increase as deuterium fluence increases. Li_2CO_3 stagnation occurs at $\sim 5.2 \times 10^{17}$ cm^{-2}, whereas Li–C–D stagnates earlier at a fluence of 2.5×10^{17} cm^{-2}. Comparing deuterium bonds in O1s and C1s for ATJ147 shows that Li–O–D saturates *after* Li–C–D stagnates (5.2×10^{17} cm^{-2} vs. 2.5×10^{17} cm^{-2}). This likely indicates that the observed Li–O–D and Li–C–D bonds are unique and are not a dual manifestation of the same functionality (shared bond) at multiple binding energies (O1s and C1s). An example of a shared bond

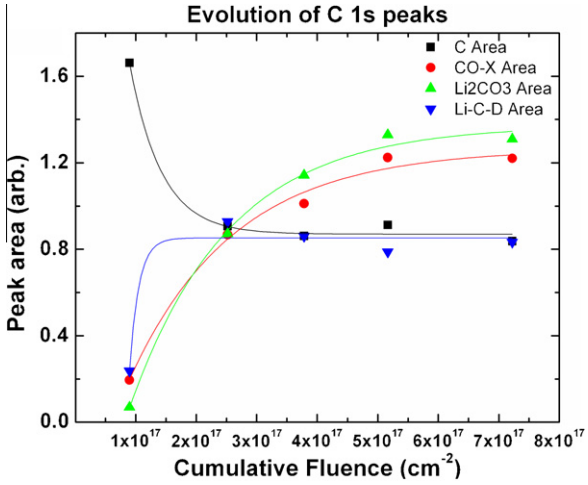

Fig. 4. Four peaks are present in the C1s spectrum after lithium deposition and deuterium irradiation. Integrated peak areas change with respect to deuterium fluence and stabilize at $\sim 5.2 \times 10^{17}$ cm^{-2}.

is CO which is visible in both the O1s photoelectron spectrum at ~532 eV and in C1s at 286.5 ± 0.6 eV. Other C1s peaks such as Li_2CO_3 and CO–X bonds continue to gain influence after Li–C–D stagnates.

3.4. Atomistic simulations of the Li, C, O, and D system

Density functional theory (DFT, GGA, 5s4p3d2f large Gaussian basis) calculations have been performed using NWChem computational chemistry package [10] for various small clusters containing Li, C, O, and H. Oxygen and carbon binding energies, relevant to the XPS measurements were considered among the lowest molecular orbitals in the optimized cluster geometry. DFT computations show that the deepest oxygen orbital electronic bonding energies in both Li–O (Li_2) and Li–O–H molecules are smaller by a few eV than unbound oxygen. Contrary, Fig. 1 shows that Li–O–D bonding occurs at 533.0 ± 0.6 eV which is higher than oxygen bonding (532.0 ± 0.6 eV), while it agrees for the Li–O peak. Likewise, computed deepest carbon binding energies in Li–C–H clusters (LiCH, $LiCH_2$, $LiCH_3$) are smaller than the deepest electronic bonding energy in free carbon. Fig. 2 shows them occurring at a higher binding energy (291.4 ± 0.6 eV). The consistency of these results for both oxygen and carbon clusters indicate that Li–D binding is much more a result of multibody attraction effects than chemical molecular bonds.

Elemental electronegativities illuminate multibody effects as it provides a quantitative representation of an atom's ability to attract a negative charge. Lithium has an electronegativity of 0.98, carbon 2.55, oxygen 3.44, and hydrogen 2.20. Because deuterium is chemically identical to hydrogen (protium) they essentially have identical electronegativities. The low electronegativity of lithium indicates its prominence of forming polar bonds with carbon, oxygen and hydrogen.

4. Conclusions

XPS analysis has been used to investigate the dynamic response of lithiated graphite to deuterium irradiation. Unique deuterium related bonds appear in the O1s spectrum as Li–O–D (533.03 ± 0.6 eV) and in the C1s spectrum as Li–C–D (292.2 ± 0.6 eV). As deuterium fluence increases, the deuterium related bonds increase in magnitude. Li–O–D is found to consume it neighboring Li–O peak indicating that Li–O is converted to Li–O–D. This effect ceases at 5.2 ± 10^{17} cm^{-2} indicating saturation. Within the C1s spectrum, the growth of Li–C–D and other carbon bonds is shown to stagnate with increasing deuterium fluence (2.5×10^{17} cm^{-2}). Five micrometer lithium is found to saturate at a higher fluence than 2 μm, however this trend does not appear to be linear at thicknesses <2 μm. Graphite devices that employ lithiumization should routinely apply coatings in excess of 2 μm. DFT computations of small free Li–O–C–D molecules and free atoms show that deuterium binding with oxygen and carbon causes the deepest electronic binding energy to shift toward lower values. In contrast, the experimental results show shifts toward stronger binding energies indicating that Li–D binding is more a result of multibody attraction of D atoms clustering around Li rather than chemical bonding.

Acknowledgements

We would like to thank Purdue University Graduate School for providing student funding, O. El-Atwani for his insight on bonding interactions, L. Kollar and T. Morton for their contributions with experiments, and D. Zemlyanov of the Birck Nanotechnology Center at Purdue University for surface analysis with the KRATOS XPS system. Work supported by US DOE Contract DE-FG02-08ER54990, DE-AC02-09CH11466.

References

[1] H.W. Kugel et al., Phys. Plasmas 15 (2008) 056118.
[2] M.G. Bell et al., Plasma Phys. Control Fusion 51 (2009) 124054.
[3] M.J. Baldwin, R.P. Doerner, S.C. Luckhardt, R.W. Conn, Nucl. Fusion 42 (2002) 1318.
[4] S.S. Harilal, J.P. Allain, A. Hassanein, M.R. Hendricks, M. Nieto-Perez, Appl. Surf. Sci. 255 (2009) 8539.
[5] C.N. Taylor, J.P. Allain, J. Appl. Phys., submitted for publication, 2010.
[6] NIST Standard Reference Database <(www.nist.gov)>.
[7] N. Itou, H. Toyoda, K. Morita, H. Sugai, J. Nucl. Mater. 290 (2001) 281.
[8] M. Nastasi, J.W. Mayer, J.K. Hirvonen, Ion-Solid Interactions, Cambridge University Press, 1996. p. 230.
[9] M. Nieto, J.P. Allain, et al., J. Nucl. Mater., these proceedings.
[10] D.E. Bernholdt et al., Int. J. Quantum Chem. 29 (1995) 475–483.